

Passive swimming in low Reynolds number flows

Piero Olla

ISAC-CNR and INFN, Sez. Cagliari, I-09042 Monserrato, Italy.

(Dated: April 23, 2022)

The possibility of microscopic swimming by extraction of energy from an external flow is discussed, focusing on the migration of a simple trimer across a linear shear flow. The geometric properties of swimming, together with the possible generalization to the case of a vesicle, are analyzed. The mechanism of energy extraction from the flow appears to be the generalization to a discrete swimmer of the tank-treading regime of a vesicle. The swimmer takes advantage of the external flow by both extracting energy for swimming and "sailing" through it. The migration velocity is found to scale linearly in the stroke amplitude, and not quadratically as in a quiescent fluid. This effect turns out to be connected with the non-applicability of the scallop theorem in the presence of external flow fields.

PACS numbers: 47.15.G-,62.25.-g,87.19.ru

One of the problems that will have to be solved in the realization of microscopic artificial swimmers ("microbots") is the energy source for locomotion. One possibility, is that of an external drive, e.g. by means of micromagnets inserted in the device [1]. The final goal, however, is that of autonomous microbots that are able to migrate, like their biologic companions, in response to external stimuli such as gradients in a chemical or temperature field.

Many situations involve swimming in a non-quiescent fluid, say the interior of a blood vessel or the neighborhood of other swimming microorganisms. These situations involve the presence of gradients in the fluid velocity and the possibility, in principle, of energy conversion from external flow to swimming. A similar idea has been put forward as regards the possibility of microscopic swimming aided by rectification of thermal fluctuations [2].

Of course, unless imagining some sort of energy storage in the microbot, the swimming velocity would be quite small, of the order of the fluid velocity difference across the device body. Nevertheless, this may be not an issue if long time or collective behaviors are sought. Examples in nature of such behaviors do exist. A most notable one is the Fahraeus-Lindwist effect: red blood cells in small arteries passively adapt their shape to the flow and align in the middle of the vessel, thus decreasing the vessel fluid-mechanic resistivity [3].

Microscopic swimming takes places in an environment dominated by viscous stresses, in which geometrical aspects play a dominant role. A strategy that has been utilized to highlight these aspects, has been to focus on systems with a minimal number of degrees of freedom. Beyond various kinds of squirmers [4], examples are the three-sphere swimmer [5, 6], the "pushmepullyou" [7] and Purcell's three-link swimmer [8, 9].

It is an easy guess that some of the geometrical constraints valid in a quiescent fluid, will cease to hold in the presence of an external flow. In particular, the scallop theorem statement [8], that reversing a sequence of deformations brings back the swimmer to its original po-

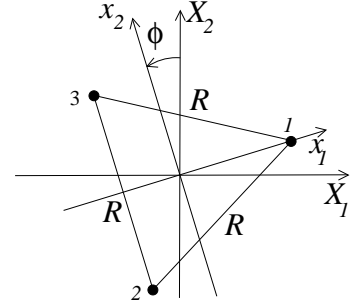


FIG. 1: The coordinate system. The bead coordinates of the undeformed trimer in the rotating frame, are $\mathbf{x}_1^{(0)}/R = (1/\sqrt{3}, 0, 0)$, $\mathbf{x}_2^{(0)}/R = -(1/(2\sqrt{3}), 1/2, 0)$, $\mathbf{x}_3^{(0)}/R = (-1/(2\sqrt{3}), 1/2, 0)$.

sition, will cease to be true.

We are going to discuss an example of device that swims extracting energy out of an external flow, based on a generalization of the three-spheres swimmer of [5] (see Fig. 1). The swimmer is placed in an unbounded linear shear flow

$$\bar{\mathbf{U}}(\mathbf{X}) = \bar{\mathbf{U}}(0) + (0, \alpha X_1, 0), \quad (1)$$

and wants to migrate along the gradient direction X_1 . We assume absence of external forces and torques on the trimer, except for those by the fluid, and neglect the interaction between the trimer arms and the fluid.

To lowest order in the ratio a/R between bead radii and arm lengths (Stokeslet approximation [10]), the contribution to the trimer dynamics from the torque on the beads by the flow is disregarded. Faxen corrections at the bead scale and higher order images from interaction of the flow perturbation with the beads are disregarded as well. In this approximation, the equation of motion for the trimer can be written in the form

$$\dot{\mathbf{X}}_i = \bar{\mathbf{U}}(\mathbf{X}_i) + \tilde{\mathbf{U}}_i(t) + \mathbf{F}_i/\sigma, \quad (2)$$

where \mathbf{X}_i is the coordinate of the i -th bead, \mathbf{F}_i is the force on bead i by the rest of the trimer, $\sigma = 6\pi\mu a$, with

μ the fluid viscosity, is the Stokes drag, and $\tilde{\mathbf{U}}_i(t)$ is the flow perturbation generated in \mathbf{X}_i by the other beads.

Contrary to the problem of the swimmer in a quiescent fluid, we see that the center of mass of the trimer $\bar{\mathbf{X}} = (\mathbf{X}_1 + \mathbf{X}_2 + \mathbf{X}_3)/3$ plays a special role, which allows, in the language of [11], to fix the gauge for the problem. In fact, absence of external forces $\sum_i \mathbf{F}_i = 0$, and linearity of the shear imply, from Eq. (2): $\bar{\mathbf{X}} = \bar{\mathbf{U}}(\bar{\mathbf{X}}) + \sum_i \tilde{\mathbf{U}}_i(t)/3$. In the absence of flow perturbation, the trimer would move as a point tracer located at its center of mass. Averaging over time the contribution by the flow perturbation gives the migration velocity of the trimer:

$$\mathbf{U}^{migr} = (1/3) \sum_i \langle \tilde{\mathbf{U}}_i \rangle. \quad (3)$$

Similar conclusions can be drawn as regards rotation around an axis passing through the swimmer center of mass. The rotation frequency $\bar{\Omega}$ can be obtained from Eq. (2) imposing absence of external torques: $\sum_i \mathbf{X}_i \times \mathbf{F}_i = 0$, that gives $\bar{\Omega} = I^{-1} \sum_i \mathbf{X}_i \times [\bar{\mathbf{U}}(\mathbf{X}_i) + \tilde{\mathbf{U}}_i(t)]$, $I = \sum_i |\mathbf{X}_i|^2$. Neglecting the effect of the flow perturbation $\tilde{\mathbf{U}}$, we find the constant rotation rate [12]:

$$\bar{\Omega}^{(0)} = \alpha/2, \quad (4)$$

that coincides with the flow vorticity (the superscript indicates order in the deformation). This a bonus from the point of view of calculation that would not be available for less symmetric shapes (for instance, in the Stokeslet approximation, a dimer would tend to align with the flow).

It is convenient to introduce a reference frame with origin in the center of mass, rotating solidly with the trimer, as illustrated in Fig. 1. Equation (4) allows to convert time averages into angular averages:

$$\langle h \rangle = \frac{1}{2\pi} \int_0^{2\pi} d\phi \left[1 + \frac{2}{\alpha} \bar{\Omega}^{(1)}(\phi) + \dots \right] h(\phi), \quad (5)$$

with ϕ the angle between the two reference frames (see Fig. 1). We shall use small case to identify vectors in the rotating frame. Equation (2) will become in this frame an evolution equation for the trimer internal degrees of freedom.

The flow perturbation produced by the trimer can be expressed in function of the forces on the beads, and, thanks to linearity of low Reynolds number hydrodynamics, the resulting relation will be linear as well; in the rotating reference frame:

$$\tilde{\mathbf{u}}_i(t) = \sum_{j \neq i} \mathbf{T}(\mathbf{x}_i, \mathbf{x}_j) \mathbf{f}_j, \quad (6)$$

where \mathbf{T} is the off-diagonal part of the Oseen tensor, relating, in the absence of an external flow, the $\dot{\mathbf{x}}_i$'s and the \mathbf{f}_j 's [10]. To lowest order in a/R , we can then write $\mathbf{T}(\mathbf{x}_i, \mathbf{x}_j) \simeq \mathbf{T}(\mathbf{x}_{ij})$, $\mathbf{x}_{ij} \equiv \mathbf{x}_i - \mathbf{x}_j$, where, for $i \neq j$ [10]:

$$\mathbf{T}(\mathbf{x}_{ij}) = \frac{3a}{4\sigma} \left[\frac{\mathbf{1}}{|\mathbf{x}_{ij}|} + \frac{\mathbf{x}_{ij} \mathbf{x}_{ij}}{|\mathbf{x}_{ij}|^3} \right]. \quad (7)$$

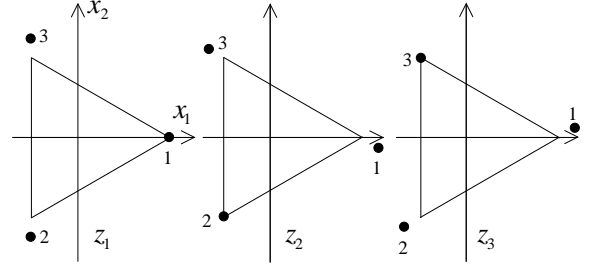


FIG. 2: Deformations of the trimer corresponding to $z_i > 0$ for $i = 1, 2, 3$. In the three cases $z_j = 0$ for $j \neq i$.

Substituting Eq. (6) into Eq. (3) and assuming exchange symmetry between the beads in the trimer:

$$\mathbf{U}^{migr} = \langle \mathbf{R} \mathbf{T}_1 \mathbf{f}_1 \rangle, \quad (8)$$

where $\mathbf{T}_1 = \mathbf{T}(\mathbf{x}_{21}) + \mathbf{T}(\mathbf{x}_{31})$ and \mathbf{R} , with $R_{11} = R_{22} = \cos \phi$, $R_{21} = -R_{12} = \sin \phi$, is the rotation matrix back to the fixed frame.

It is easy to see that a rigid trimer, due to the symmetry of its shape and of the external flow, would be unable to migrate. We must consider deformations.

We can express the trimer deformation in terms of three independent parameters z_1, z_2, z_3 as follows:

$$\begin{aligned} \mathbf{x}_1^{(1)}/R &= ((\sqrt{3}/2)(z_2 + z_3), (z_3 - z_2)/2, 0), \\ \mathbf{x}_2^{(1)}/R &= (-\sqrt{3}/2 z_3, -z_1 - z_3/2, 0), \\ \mathbf{x}_3^{(1)}/R &= (-\sqrt{3}/2 z_2, z_1 + z_2/2, 0). \end{aligned} \quad (9)$$

As illustrated in Fig. 2, positive z_i corresponds to stretching of the arm opposite to bead i . From Eq. (8), to determine \mathbf{U}^{migr} , we must calculate \mathbf{f}_1 at least to $O(z)$, $z = (\sum_i z_i^2)^{1/2}$, but we can neglect the effect of the field perturbation. The rotating frame version of Eq. (2) reads at $O((a/R)^0)$: $\mathbf{f}_i/\sigma = \dot{\mathbf{x}}_i - \bar{\mathbf{u}}(\mathbf{x}_i)$.

At $O(z^0)$ there are no deformations and $\dot{\mathbf{x}}^{(0)} = 0$. To next order, from Eq. (5), we can write $\dot{\mathbf{x}}^{(1)} = (\alpha/2) \mathbf{x}^{(1) \prime}$ with prime indicating $d/d\phi$. From Eq. (4), the rotation velocity equals to $O(z^0)$ the vorticity of the field; hence $\bar{\mathbf{u}}^{(0)}$ is purely due to strain, $\bar{\mathbf{u}}^{(0)}(\mathbf{x}) = \bar{\mathbf{S}} \mathbf{x}$, with

$$\bar{S}_{11} = -\bar{S}_{22} = \frac{\alpha}{2} \sin 2\phi, \quad \bar{S}_{12} = \bar{S}_{21} = \frac{\alpha}{2} \cos 2\phi. \quad (10)$$

At $O(z)$, $\bar{\mathbf{u}}$ receives a vorticity components from the correction to the trimer rotation velocity: $\bar{\mathbf{u}}^{(1)}(\mathbf{x}) = -\bar{\Omega}^{(1)} \times \mathbf{x}$. To $O(z)$ the trimer evolution equation will read therefore

$$\mathbf{f}_i^{(0)} = -\sigma \bar{\mathbf{S}} \mathbf{x}_i^{(0)}, \quad (11)$$

$$\mathbf{f}_i^{(1)} = \sigma [(\alpha/2) \mathbf{x}_i^{(1) \prime} - \bar{\mathbf{S}} \mathbf{x}_i^{(1)} + \bar{\Omega}^{(1)} \times \mathbf{x}_i^{(0)}]. \quad (12)$$

To obtain $\bar{\Omega}^{(1)}$, we apply $\mathbf{x}_i^{(0)} \times$ at both sides of Eq. (12) and sum over i , with the result $\bar{\Omega}^{(1)} = \sum_i \mathbf{x}_i^{(0)} \times \bar{\mathbf{S}} \mathbf{x}_i^{(1)} / I^{(0)}$,

$I^{(0)} = \sum_i |\mathbf{x}_i^{(0)}|^2 = R^2$. Direct calculation from Eqs. (9-10) gives then

$$\bar{\Omega}^{(1)} = \left[\sqrt{3}(z_2 - z_3) \sin 2\phi + (z_2 + z_3 - 2z_1) \cos 2\phi \right] \frac{\alpha}{4}. \quad (13)$$

Substituting Eqs. (5,7) and (9-13) into Eq. (8), we find the lowest order contribution $\mathbf{U}^{migr} \simeq \langle \mathbf{R}(\mathbf{T}_1^{(0)} \mathbf{f}_1^{(1)} + \mathbf{T}_1^{(1)} \mathbf{f}_1^{(0)}) \rangle^{(0)}$, where $\langle \cdot \rangle^{(0)}$ indicates the uniform part of the average in Eq. (5). Imposing exchange symmetry among the beads:

$$z_i = \sum_n [A_n \cos n\phi_i + B_n \sin n\phi_i], \quad (14)$$

where $\phi_1 = \phi$, $\phi_{2,3} = \phi \mp 2\pi/3$. We see that Eqs. (5,10,13) bring into Eq. (8) factors $\cos 2\phi$ and $\sin 2\phi$ that combined with the $\cos \phi$ and $\sin \phi$ in \mathbf{R} , require, for a non zero migration velocity, contributions $\propto \cos \phi, \cos 3\phi, \sin \phi, \sin 3\phi$ in the deformation. Direct calculation, using $T_1^{11} \simeq \beta\{7/2 - [13z_1 + 29(z_2 + z_3)]/8\}$, $T_1^{12} = T_1^{21} \simeq \beta(\sqrt{3}/8)(z_2 - z_3)$ and $T_1^{22} \simeq \beta\{5/2 + [2z_1 - 31(z_2 + z_3)]/8\}$, $\beta = 3a/(4\sigma R)$, together with Eq. (14), gives in fact the result:

$$U_1^{migr} \simeq -\frac{\sqrt{3}\alpha a}{256} [73B_1 + 13B_3]. \quad (15)$$

The component B_1 corresponds to the pulsation regime depicted in Fig. 3. From here, the swimming strategy could be optimized minimizing at fixed U_1^{migr} the deformation amplitude z or some more appropriate cost function [13].

Notice that, of all the contributions to migration, perhaps, only the one coming from the first term to right hand side of Eq. (12) qualifies as real swimming. It is in fact the only direct contribution from deformation to bead movement with respect to the fluid. All the others could be loosely described as a sort of sailing, in which the swimmer shape adapts to catch the external flow.

The way the swimmer actually swims, is illustrated in Fig. 3. We see that propulsion does not come from direct drag by $\bar{\mathbf{U}}$, rather, from drag by the perturbation $\tilde{\mathbf{U}}$ generated by interaction between the trimer and the external flow. Imposing exchange symmetry among the beads, allows, on the same line of Eq. (8), to focus on the Stokeslet field of a single bead, say bead 1. Let us consider the contribution $B_1 \sin \phi_1$. We see that the Stokeslet field generated by bead 1 in response to the strain component of $\bar{\mathbf{U}}$, has a positive or negative component at beads 2, 3, depending on whether $0 < \phi < \pi$ or $\pi < \phi < 2\pi$. Migration is produced by the deformation induced symmetry breaking between the two orientations.

The swimmer of Eq. (14) behaves as a small engine, with the three arms stretching and contracting in sequence. From linearity in z of U_1^{migr} , however, migration in the symmetric case of Eq. (14), implies migration also in the presence of a single deformable link. The scallop theorem does not apply in the present situation: the swimmer orientation and position are determined jointly

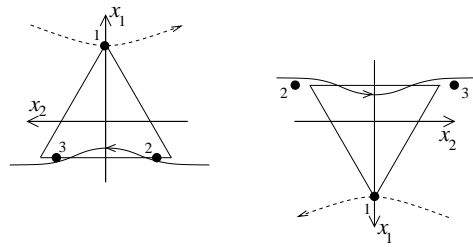


FIG. 3: The swimming strategy. When $\phi = \pi/2$ (left), arm 23 contracts, which turns out to maximize the drag along X_1 by bead 1's Stokeslet field [continuous line; see Eq. (7)]. The opposite occurs for $\phi = -\pi/2$ (right). Dashed lines identify the strain component of $\bar{\mathbf{U}}$.

by the past history of deformations and of the gradients of $\bar{\mathbf{U}}$ experienced: even correcting for the trivial displacement by $\bar{\mathbf{U}}$, reversing the deformations only, would not be sufficient to bring the trimer back to its original position. Similar "violations" of the scallop theorem have been observed in [14], where the role of external flow was played by the perturbation generated in the fluid by other swimmers.

This situation has a counterpart in the fact that swimming in an external flow occurs already at $O(z)$, and not at $O(z^2)$. The swimmer achieves this, exploiting the external flow to change orientation between reversed strokes; in a quiescent fluid, the orientation change would require other stroke components, and this is responsible for $O(z^2)$ swimming efficiency [11].

It is actually possible for the swimmer to extract the energy needed for migration directly from the external flow. The average power exerted by the swimmer on the fluid is $\dot{W} = 3\langle \dot{\mathbf{x}}_1 \cdot \mathbf{f}_1 \rangle$. Now, from $\dot{\mathbf{x}}_i^{(0)} = 0$, the first contribution is $\dot{W}^{(1)} = 3\langle \dot{\mathbf{x}}_1^{(1)} \cdot \mathbf{f}_1^{(0)} \rangle^{(0)}$, but the $\mathbf{x}^{(1)}$ components contributing to swimming, entering Eq. (15), are odd in ϕ , while $\mathbf{f}_i^{(0)}$, from Eq. (11), is even. The same occurs, from Eqs. (5) and (13), with $\langle \cdot \rangle^{(1)}$. Assuming that $\mathbf{x}^{(1)}$ receives contributions only from $B_{1,3}$, the lowest order contribution to the power will be

$$\dot{W}^{(2)} = 3[\langle \dot{\mathbf{x}}_1^{(1)} \cdot \mathbf{f}_1^{(1)} \rangle^{(0)} + \langle \dot{\mathbf{x}}_1^{(2)} \cdot \mathbf{f}_1^{(0)} \rangle^{(0)}]; \quad (16)$$

we see that choosing $\mathbf{x}^{(2)}$ in appropriate way, we could set $\dot{W}^{(2)} = 0$, compensating to $O(z^2)$ the energy lost in swimming. From Eq. (11), the only terms in $\mathbf{x}^{(2)}$ contributing to $\dot{W}^{(2)}$ are $\propto \cos 2\phi, \sin 2\phi$. Substituting Eqs. (9,11,14) into Eq. (16) we obtain:

$$A_2 > \frac{3\sqrt{3}}{32} (B_1^2 - 5B_1B_3 + 36B_3^2), \quad (17)$$

where the inequality accounts for the internal dissipation of the device [at this point the condition that $A_2 = O(z^2)$ becomes irrelevant]. Looking at Fig. 3 and focusing again on bead 1, we see that this deformation corresponds to arm 23 being stretched when it is parallel to the flow direction, and contracted when it is perpendicular. Energy extraction from the flow comes from the fact that

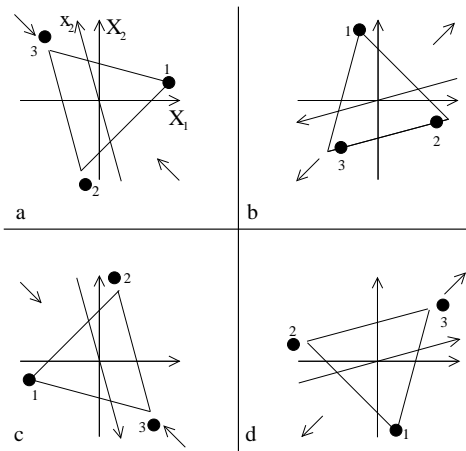


FIG. 4: Swimming from braking. Suppose \mathbf{x}_{23} enters the contracting quadrants in a stretched state (a). The brake is relaxed and the arm contracts, till it enters the stretching quadrants fully contracted (b). The brake remains off till the arm returns, now fully stretched, into the contracting quadrants (c). At this point, the brake is acted on and $|\mathbf{x}_{23}|$ remains stretched until, passing through (d), it returns to (a).

the $|\mathbf{x}_{23}|$ grows in the stretching quadrants of the external strain, and decreases in the contracting ones (see Fig. 3).

What mechanism could allow a three-sphere swimmer, such as the one described, to passively undergo the deformation sequence depicted in Eqs. (15) and (17)? A possibility is illustrated in Fig. 4: a system of orientation dependent brakes, controlling the stretching and contraction of the trimer arms in response to the external strain (a more quantitative description of this mechanism is provided in [15]). This mechanism contains all the required

aspects of conversion of external flow to deformation and then to swim. We notice the asymmetry between the two configurations (b) and (d), that is necessary to migration. At the same time, comparing orientations (a) and (c) with (b) and (d), we see that arm 23 is in the stretched state when aligned with $\bar{\mathbf{U}}$, meaning that energy is extracted from the external flow.

All the behaviors that have been described, derive from geometrical properties of the swimmer and could be expected to remain valid away from the small deformation regime considered. More importantly, it should be possible to construct a continuous counterpart of the trimer, for which the migration velocity predictions of Eq. (15) remain qualitatively valid, albeit substitution between the typical size of the moving parts in the two situations: $a \rightarrow R$. Such a continuous swimmer should have the properties imposed by Eqs. (15) and (17): an overall shape in the laboratory frame that is stretched along $\bar{\mathbf{U}}$ and asymmetric; say an egg with the tip pointing at positive X_2 . In other words, a tank-treading cell [16, 17] with a fixed orientation asymmetric shape. Unfortunately, this would require an orientation sensitive control of the device structure (compare with Fig. 4), and the practical realization of such a device at the microscale would be very difficult.

Nevertheless, from a conceptual point of view, some complex version of tank-treading appears to be the most effective strategy for a swimmer to exploit the presence of an external flow. A linear swimmer, say, could very well extract energy from $\bar{\mathbf{U}}$ in a tumbling cycle, and use it to generate swimming strokes as if in a quiescent fluid. However, beyond having a lower stroke frequency than a comparable triangular device (it would spend most of the time aligned with the flow), it would have only quadratic efficiency in the stroke amplitude.

-
- [1] R. Dreyfus, J. Baudry, M.L. Roper, M. Fermigier, H.A. Stone and J. Bibette, *Nature* **437**, 862 (2005); M. Leoni, J. Kotar, B. Bassetti, P. Cicuti, M.C. Lagomarsino, *Soft Matter* **5**, 472 (2009)
 - [2] V. Lobaskin, D. Lobaskin and I.M. Kulic, *Eur. Phys. J. Special Topics* **157**, 149 (2008); R. Golestanian and A. Ajdari, *J. Phys. Condens. Matter* **21**, 204104 (2009)
 - [3] V. Vand, *J. Phys. Chem.* **52**, 277 (1948)
 - [4] M.J. Lighthill, *Commun. Pure Appl. Math.* **5**, 109 (1952); B.U. Felderhof and R.B. Jones, *Physica A* **202**, 119 (1994); H.A. Stone and A.D.T. Samuel, *Phys. Rev. Lett.* **77**, 4102 (1996); T. Ishikawa and T.J. Pedley, *Phys. Rev. Lett.* **100**, 088103 (2008)
 - [5] A. Najafi and R. Golestanian, *Phys. Rev. E* **69**, 062901 (2004)
 - [6] C.M. Pooley, G.P. Alexander and J.M. Yeomans, *Phys. Rev. Lett.* **99**, 228103 (2007)
 - [7] J.E. Avron, O. Kenneth and D.K. Oaknin, *New J. Phys.* **7**, 234 (2005)
 - [8] E.M. Purcell, *Am. J. Phys.* **45**, 3 (1977)
 - [9] L.E. Becker, S.A. Koehler and H.A. Stone *J. Fluid Mech.* **490**, 15 (2003)
 - [10] J. Happel and H. Brenner, *Low Reynolds number hydrodynamics* (Kluwer, Boston, 1973)
 - [11] A. Shapere and F. Wilczek, *J. Fluid Mech.* **198**, 557 (1989)
 - [12] It can be shown that a device formed by four beads at the vertices of a regular tetrahedron will share this property, irrespective of its initial orientation.
 - [13] J.E. Avron, O. Gat and O. Kenneth, *Phys. Rev. Lett.* **93**, 186001 (2004)
 - [14] G.P. Alexander, C.M. Pooley and J.M. Yeomans, *Phys. Rev. E* **78**, 045302(R) (2008); E. Lauga and D. Bartolo, *Phys. Rev. E* **78**, 030901(R) (2008)
 - [15] P. Olla 2010 *Preprint* arXiv:1004.4179
 - [16] S.R. Keller and R. Skalak, *J. Fluid Mech.* **120**, 27 (1982)
 - [17] G. Couplier, B. Kaoui, T. Podgorski and C. Misbah, *Phys. Fluids* **20**, 111702 (2008)